https://doi.org/10.5194/essd-2026-204
Preprint. Discussion started: 1 April 2026
© Author(s) 2026. CC BY 4.0 License.

Open Access Earth System Science Data Discussions

HDM-Plot: a plot dataset of plant communities across three-dimensional zonal vegetation in the Hengduan Mountains, southwestern China

Yili Jin, Liuyiyi Yang, Xiaofei Hu, Chen Yang, Haojun Xia, Ying Hou, Kai Wu, Shaolin Shi, Xingxing Mao, Jian Ni

College of Life Sciences, Zhejiang Normal University, Jinhua 321004, China

Correspondence: Xingxing Mao (xyz1314@zjnu.edu.cn); Jian Ni (nijian@zjnu.edu.cn).

Abstract. The Hengduan Mountains (HDM) constitute one of the world's richest biodiversity regions and are designated as a top-tier priority for ecological conservation. Vegetation investigations can help with the design and implementation of biodiversity conservation in this region. Here we present the HDM-Plot, a plot-based vegetation dataset compiled from 314 plots surveyed during four campaigns between 2022 and 2024, spanning major vegetation types from lowland dry-hot valleys to alpine areas in altitudes of 754–4,932 m. Each plot records detailed species-level information, including scientific name, growth form, life form, abundance, plant height, diameter at breast height or at base, crown width, and coverage, along with geographic coordinates and hierarchical vegetation classification. In total, the dataset comprises 14,113 individual records belonging to 1,127 species from 379 genera and 117 families. The dominant families are Rosaceae (133 species), Ericaceae (93), Fabaceae (66), Asteraceae (63), and Fagaceae (37), and the dominant genera are *Rhododendron* (75), *Berberis* (34), *Cotoneaster* (30), *Salix* (24), and *Quercus* (22), with composition varying among vegetation types. Growth forms are mainly composed of shrubs (46.0%), trees (27.3%), and herbs (23.6%). Herbs are dominated by perennial (92.1%), shrubs are mainly deciduous broadleaf (59.7%), and trees are primarily deciduous broadleaf (46.8%) and evergreen broadleaf (41.6%). Species richness exhibits a unimodal pattern with a mid-elevation peak, while growth forms and life forms show clear elevational changes. Floristically, temperate (54.1%) and tropical (35.4%) areal-types are predominant. 314 plots can be assigned to three vegetation formation groups, 18 vegetation formations, 142 alliance groups, 209 alliances, 238 association groups, and 299 associations. The HDM-Plot dataset provides an updated and standardized baseline for quantitative analyses of mountain vegetation, biodiversity assessment, and vegetation classification and mapping in southwestern China. Such information can be future used in the revisions of China's vegetation classification scheme and *Vegegraphy of China*. The

https://doi.org/10.5194/essd-2026-204
Preprint. Discussion started: 1 April 2026
© Author(s) 2026. CC BY 4.0 License.

dataset is available through the National Tibetan Plateau / Third Pole Environment Data Center (Jin et al., 2026; https://doi.org/10.11888/Terre.tpdc.303394).

1 Introduction

The Hengduan Mountains (HDM) form the core mountainous region in southwestern China and are recognized as one of the world's richest biodiversity hotspots and a global priority area for ecological conservation (Myers et al., 2000; Sloan et al., 2014). Located at the junction between the Tibetan Plateau and the Yangtze Block, the HDM represents a young and rapidly evolving orogenic belt shaped by ongoing tectonic uplift associated with Indian–Eurasian collision (Xing and Ree, 2017). Long-term mountain uplift, together with intense river incision, has generated exceptional topographic complexity, characterized by closely spaced north–south–oriented high mountains and deeply incised valleys (Integrated Scientific Expedition to Qinghai-Tibet Plateau, Chinese Academy of Sciences, 1997). As an ecotonal region linking subtropical lowlands to alpine highlands, the HDM is affected by the southwest and southeast monsoons as well as mesoscale atmospheric systems (Wu et al., 2012; Zhang et al., 2024). These interacting geological and climatic processes create strong environmental heterogeneity, supporting abundant biodiversity, significant spatial differentiation of ecosystems, and complex vegetation distribution (Liang et al., 2018; Ding et al., 2020; He et al., 2020). Consequently, robust characterization of species composition, community structure, and vegetation zonation in the HDM is essential for biodiversity conservation and sustainable development, thereby provides key empirical support for advancing studies of global mountain biogeography and ecology.

Vegetation represents the most visible and distinctive ecological feature of a region, and plot-based plant community data provide the fundamental basis for documenting vegetation composition and distribution patterns, as well as for the compilation of the *Vegegraphy*—a series of monographs that describe detailed species composition, structures, functions, environmental settings, and distribution of a set of plant communities and/or their combinations for each vegetation type, using community data

https://doi.org/10.5194/essd-2026-204
Preprint. Discussion started: 1 April 2026
© Author(s) 2026. CC BY 4.0 License.

from vegetation survey (Fang et al., 2020; Wang et al., 2020; Sabatini et al., 2021). Over recent decades, extensive vegetation surveys have been conducted across the HDM, including those in the First (1970–1990) and Second (2018–2024) Tibetan Plateau Scientific Expeditions, and numerous regional surveys (the late 20th to the early 21st Century). These efforts have substantially advanced theoretical knowledge of floristic composition (Li, 1988; Shen et al., 2004; Xu et al., 2014; Yu et al., 2020), community structure (Sherman et al., 2008; Xu et al., 2008; Sun et al., 2017), vegetation distribution (Yao et al., 2010; Liang et al., 2018; Wu and Yu, 2020; Zhang et al., 2023), eco-geographical regionalization (Zheng and Yang, 1987; Yang and Zheng, 1989; Chi et al., 2019), and vegetation modeling (He et al., 2020; Yin et al., 2020), with sustained attention to dry-hot valley vegetation (Jin and Ou, 2000; Jin, 2002; Liu et al., 2016a, b; Yang J D et al., 2016; Yang Y et al., 2016).

Existing plot surveys consistently indicate significant horizontal differentiation and elevational turnover in HDM vegetation (Editorial Committee of Vegetation Map of China, the Chinese Academy of Sciences, 2007a, b). Vegetation across the HDM spans three regions in the vegetation regionalization scheme of China: the dominated one is the subtropical evergreen broadleaf forest region, while a small area in the northwestern sector is transitioned to the Qinghai-Xizang Plateau alpine vegetation region, and the western margin is the tropical monsoon rain forest and rain forest region (Fig. 1; Editorial Committee of Vegetation Map of China, the Chinese Academy of Sciences, 2007b). From the southeast toward the northwest, vegetation shifts from subtropical evergreen broadleaf forests and dry-hot valley shrubby grasslands to subalpine shrublands and alpine meadows (Fig. 1; Editorial Committee of Vegetation Map of China, the Chinese Academy of Sciences, 2007a). Along elevational gradients, vegetation belt spectra typically transition from dry-hot valley shrubland belt through the belts of mountains evergreen broadleaf forest, mixed needleleaf and broadleaf forest, and needleleaf forest, to the belts of alpine shrubland and meadow, alpine meadow, and the nival (Fig. 1; Zheng, 1988). Despite a large number of community plot data accumulated by earlier surveys, many datasets remain difficult to integrate for synthesis due to extended temporal spans, limited accessibility of original records, heterogeneous

https://doi.org/10.5194/essd-2026-204
Preprint. Discussion started: 1 April 2026
© Author(s) 2026. CC BY 4.0 License.

Open Access Earth System Science Data Discussions

study designs, as well as inconsistent taxonomic and classification frameworks across campaigns. Meanwhile, vegetation in the HDM has been reshaped under increasing climate change and human activities (Zhang et al., 2015; Piao et al., 2019), highlighting the need for updated, standardized, and openly available plot-based plant community data.

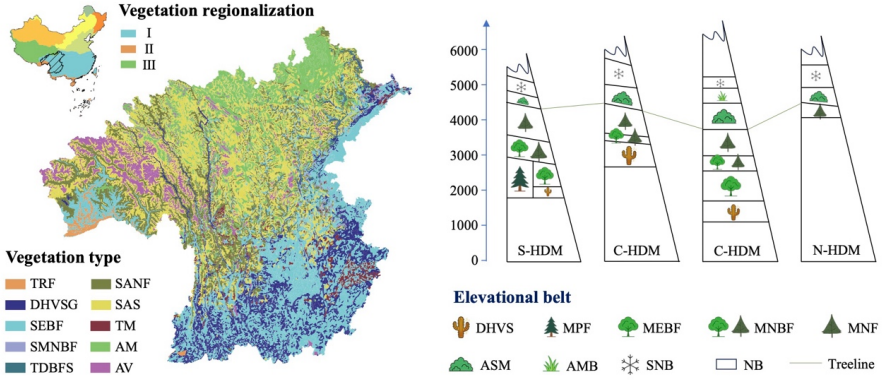

Figure 1. Spatial patterns of vegetation in the Hengduan Mountains (HDM). The upper-left inset map shows the location of the HDM in China and the vegetation regionalization from the *Vegetation Regionalization Map of China* (Editorial Committee of Vegetation Map of China, the Chinese Academy of Sciences, 2007b). I, subtropical evergreen broadleaf forest region; II, tropical monsoon rain forest and rain forest region; and III, Qinghai-Xizang Plateau alpine vegetation region. The left panel exhibits the vegetation types extracted from the *1:1,000,000 Vegetation Map of the People's Republic of China* (Editorial Committee of Vegetation Map of China, the Chinese Academy of Sciences, 2007a). The original 35 vegetation formations were aggregated into 10 categories based on climatic zones, community structures, and ecological function. TRF, tropical rain forest; DHVSG, dry-hot valley shrubby grassland; SEBF, subtropical evergreen broadleaf forest; SMNBF, subtropical mountains mixed needleleaf and broadleaf forest; TDBFS, temperate deciduous broadleaf forest and shrubland; SANF, subalpine needleleaf forest; SAS, subalpine shrubland; TM, temperate meadow; AM, alpine meadow; AV, alpine cushion and sparse vegetation, and bare land. The right panel presents elevational belts (revised after Zheng, 1988) for the southern (S-HDM), central (C-HDM) and northern (N-HDM) sectors. DHVS, dry-hot valley shrubland belt; MPF, mountains *Pinus* forest belt; MEBF, mountains evergreen broadleaf forest belt; MNBF, mountains mixed needleleaf and broadleaf forest belt; MNF, mountains needleleaf forest belt; ASM, alpine shrubland and meadow belt; AMB, alpine meadow belt; SNB, subnival belt; NB, nival belt.

To provide an up-to-date baseline of vegetation composition and spatial patterns in the HDM, we conducted four large-scale surveys between 2022 and 2024 along the major mountains and valleys, spanning tropical, subtropical, and temperate zones and extending into subalpine and alpine environments, in accordance with the horizontal

https://doi.org/10.5194/essd-2026-204
Preprint. Discussion started: 1 April 2026
© Author(s) 2026. CC BY 4.0 License.

and vertical zonation. We surveyed 314 plant community plots and integrated all field records into a standardized plot-based vegetation dataset, HDM-Plot. It documents plant species composition and taxonomic attributes and supports a consistent vegetation classification across the region. The HDM-Plot dataset provides a contemporary and standardized baseline for plant community study and long-term monitoring of vegetation, and serves as a vital reference for biodiversity conservation, vegetation restoration, and sustainable development. It also offers empirical support for revising of the China's vegetation classification scheme (Guo et al., 2020) and the compilation of the *Vegegraphy of China* (Fang et al., 2020).

2 Study area

The HDM cover a broad geographical extent, and their spatial boundaries can vary slightly among studies depending on research objectives. Here we define the HDM as extending from 24.08º to 34.32º N and from 93.13º to l06.16º E, with elevations ranging from 119 to 7,213 m (Fig. 2), following the standard of two studies (Yu et a., 1989; Zhang et al., 1997). The region exhibits an overall increase in elevation from the southeast toward the northwest and is characterized by a series of north–south–oriented mountains and deeply incised valleys. Climatically, the HDM span tropical, subtropical, temperate, and alpine zones, with mean annual temperature ranging from –18.2 to 25.1 °C. Warmer conditions are concentrated in the dry-hot valleys and lower subtropical mountains in the southeast, and in the tropical rainforests along the western margin, while much lower temperatures occur across the highlands toward the northwest. Mean annual precipitation across the region varies but is generally lower (0–1,793 mm), and relatively humid conditions are mainly associated with the southwestern and southeastern margins (Fig. 2).

https://doi.org/10.5194/essd-2026-204
Preprint. Discussion started: 1 April 2026
© Author(s) 2026. CC BY 4.0 License.

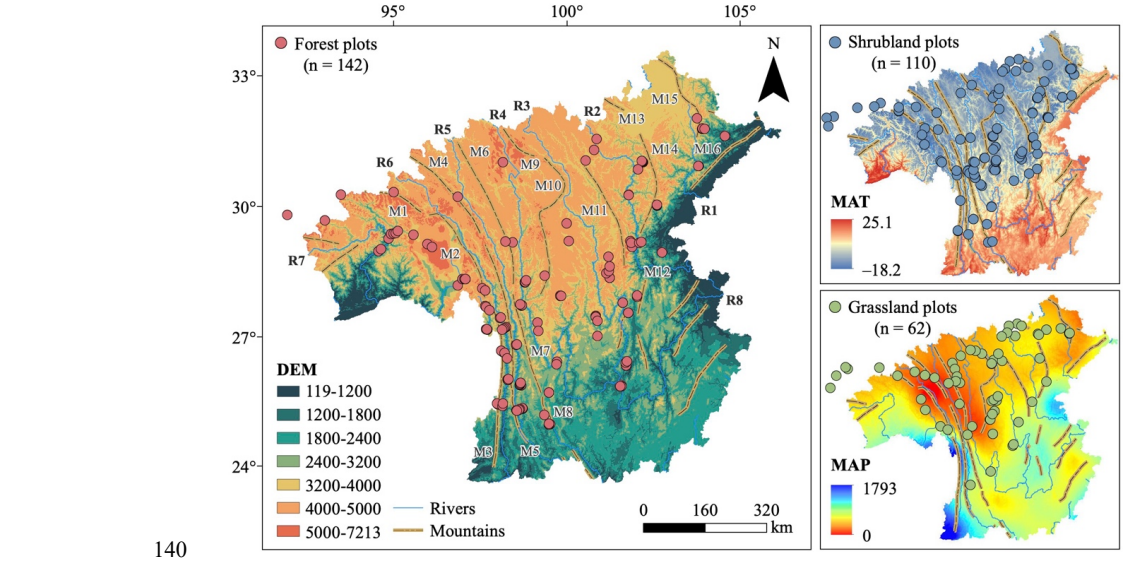

Figure 2. Distribution of vegetation plots in the Hengduan Mountains. Vegetation plots of different vegetation types (forest, shrubland, and grassland), often overlapped in one location, were separately drawn on different maps. n indicates the number of plots. Digital elevation model (DEM, m) was derived from the SRTM 90 m dataset (Farr et al., 2007) and resampled into 1 km grid cells. Mean annual temperature (MAT, °C) and mean annual precipitation (MAP, mm) were derived from the monthly climatological standard normals at 2,152 meteorological stations across China in 1981–2010 (China Meteorological Data Service Centre, http://data.cma.cn, last access: 8 June 2024), and interpolated into 1 km grid cells by using the thin-plate smoothing spline in ANUSPLIN version 4.4. Mountain data were extracted from the Digital Mountain Map of China Dataset (Nan et al., 2015). Major mountains include: M1, Nyenchen Tanglha Mountain (Mt); M2, Boshulaling Mt; M3, Gaoligong Mt; M4, Taniantaweng Mt; M5, Nushan Mt; M6, Mangkang Mt; M7, Yunling Mt; M8, Diancang Mt; M9, Que'er Mt; M10, Shaluli Mt; M11, Daxue Mt; M12, Xiaoxiangling Mt; M13, Bayan Har Mt; M14, Qionglai Mt; M15, Minshan Mt; and M16, Longmen Mt. River data were extracted from the Natural Earth (https://www.naturalearthdata.com, last access: 12 March 2026). Major rivers include: R1, Min River; R2, Dadu River; R3, Yalong River; R4, Jinsha River; R5, Lancang River; R6, Nu River; R7, Yarlung Tsangpo River; and R8, Yangtze River.

3 Materials and Methods

3.1 Vegetation survey

Field surveys were conducted during four campaigns in March 2022, May–June 2022, May–June 2023, and June 2024. May–June was selected as the primary survey time because most species across elevational belts in the region have developed diagnostic vegetative structures and even many have begun flowering, enabling reliable

https://doi.org/10.5194/essd-2026-204
Preprint. Discussion started: 1 April 2026
© Author(s) 2026. CC BY 4.0 License.

identification. In addition, it coincides with the transition from the dry to the wet season when precipitation is still relatively low and field accessibility is generally high. An additional survey in March 2022 targeted dry-hot valley vegetation, where phenological development occurs earlier under warm and relatively arid conditions.

To capture the major vegetation belts and transition zones shaped by the regional mountain–valley and climatic system, plots were set up across representative mountains and valleys of the HDM along longitudinal, latitudinal, and elevational gradients, with logistics and road accessibility considered. Plot size was determined following community physiognomy and stand heterogeneity. Forest plots were typically 10 m × 10 m to 20 m × 20 m, shrubland plots 2 m × 2 m to 10 m × 10 m, and grassland plots 1 m × 1 m to 2 m × 2 m. In forest and shrubland plots, all woody species were recorded, including species name, growth form, phenological period, abundance, height, stem diameter, and crown width. Diameter was generally measured as diameter at breast height (DBH). For individuals < 2 m tall or when DBH was not applicable, basal diameter was recorded. In forest plots, individuals with height ≥ 5 m were assigned to the tree layer, whereas shrubs and tree seedlings with height < 5 m were classified into the shrub layer. In grassland plots, all herbaceous species were recorded, including species name, growth form, phenological period, abundance, maximum leaf-layer height, and coverage.

For each plot, longitude, latitude, elevation, community height and total coverage, as well as disturbance intensity were recorded. The global position system was used to determine the geographic coordinates. Community height and coverage were visually estimated in the field. Disturbance intensity was assessed directly at four levels: none, weak, medium, and strong. In total, 314 plots were surveyed, belonging to 142 forest plots, 110 shrubland plots, and 62 grassland plots (Fig. 2; Table 1).

Table 1 Summary statistics of plots in the HDM-Plot dataset

Plot	All	Forest	Shrubland	Grassland
Number of plots	314	142	110	62
Longitude (°E)	92.055–104.581	92.661–104.581	92.055–103.941	92.325–103.771

https://doi.org/10.5194/essd-2026-204
Preprint. Discussion started: 1 April 2026
© Author(s) 2026. CC BY 4.0 License.

Latitude (°N)	25.547–33.077	25.547–32.749	25.557–33.065	26.423–33.077
Elevation (m)	754–4932	754–4377	1144–4758	3168–4932
SR (species / plot)	1–37	2–37	1–22	3–24
	(11 ± 6)	(13 ± 7)	(6 ± 4)	(12 ± 5)
Height (m)	0.001–49.0	5.2–49.0	0.1–10.0	0.001–0.500
	(8.238 ± 8.982)	(16.0 ± 7.8)	(2.8 ± 2.2)	(0.081 ± 0.079)
Coverage (%)	10–100	35–100	10–100	15–100
	(71 ± 18)	(71 ± 15)	(66 ± 20)	(79 ± 18)
Number of families	117	91	53	38
Number of genera	379	239	124	114
Number of species	1127	737	321	266

Values for species richness (SR), community height, and coverage are presented as ranges, with mean ± SD in parentheses.

3.2 Data processing and analysis

Species were identified following national and regional floras, including the *Flora Republicae Popularis Sinicae* (Editorial Committee of Flora of China, Chinese Academy of Sciences, 1959–2004), *Flora of Yunnan* (Kunming Institute of Botany, Chinese Academy of Sciences, 1977–2006), *Flora Xizangica* (Integrated Scientific Expedition to Qinghai-Tibet Plateau, Chinese Academy of Sciences, 1983–1987), and *Flora of Sichuan* (Gao et al., 1981). Final species names were then standardized and validated against the iPlant online taxonomic system (http://www.iplant.cn/, last access: 16 January 2026). In the most recent taxonomy system of *Flora of Pan-Himalaya* (Zhang, 2010), *Kobresia* is classified into *Carex*. Given the ecological importance of *Kobresia* in alpine zonal vegetation, and in order to maintain consistency with vegetation literatures, we retained *Kobresia* as a traditional genus name for data analyses, while the dataset provides both names.

Growth forms were classified from field observations following the definitions in *Vegetation of China* (Editorial Committee of the Vegetation of China, 1980) into tree, shrub, climber, semi-shrub, and herb. Some taxa (e.g., *Quercus* and *Rhododendron*) can

https://doi.org/10.5194/essd-2026-204
Preprint. Discussion started: 1 April 2026
© Author(s) 2026. CC BY 4.0 License.

Open Access Earth System Science Data Discussions

shows both shrubs and small trees, and they were recorded at the plot level according to the observed status. For regional summary analyses, each species was additionally assigned a single predominant growth form based on its most frequent form seen in the field across the dataset. Woody species were further divided by leaf type (needleleaf vs. broadleaf) and phenology (evergreen vs. deciduous). Herbaceous species were categorized into annual, biennial, and perennial life forms. Floristic areal-types of plant families and genera were assigned primarily based on the *Areal-types of the World Families* and *Chinese Genera of Seed Plants* (Wu et al., 1991, 2003), supplemented by the *Floristic Statistics and Analyses of Seed Plant from China* (Li, 1996) and *Dictionary of the Families and Genera of Chinese Vascular Plants* (iFlora Initiative of Kunming Institute of Botany, Chinese Academy of Sciences, 2018).

Vegetation classification followed the *revised scheme of vegetation classification system of China* (Guo et al., 2020), which adopted a three-level hierarchy (vegetation formation, alliance, and association) and emphasizes constructive and dominant species in reflecting the primary structural characteristics of plant communities. For each level, a corresponding supplementary classification unit was defined (vegetation formation group, alliance group, and association group). Dominance was identified using species importance value (IV, %) calculated following Fang et al. (2009): for tree-layer species, IV combined relative abundance, relative height, and relative basal area; for shrub-layer species, IV combined relative abundance and relative height; and for herb-layer species, relative abundance and relative coverage, with relative metrics as the percentages of a plot total. A community was assigned a single dominant species when one species had IV > 75%. When multiple species showed IV between 10% and 75%, species were designated as dominant and sub-dominant in descending order of IV if interspecific IV differences exceeded 10%, and as co-dominant when IV differences were ≤ 10%. When all species had IV < 10%, the community was treated as lacking a clear dominant species, and thereby species were simply ranked by IV (Wang et al., 2020). Vegetation formation groups were defined by community ecological physiognomy (e.g., forests), and vegetation formations by the life form of the constructive species (e.g., evergreen needleleaf forests). Alliance groups were divided by the genus of constructive species

https://doi.org/10.5194/essd-2026-204
Preprint. Discussion started: 1 April 2026
© Author(s) 2026. CC BY 4.0 License.

(e.g., *Abies* forest alliance group), and alliances by the constructive species (e.g., *A. georgei* forest alliance). Association groups were identified by the constructive species together with the life form of sub-dominant species (e.g., *A. georgei* - shrub forest association group), and associations were determined by the constructive species and sub-dominant species (*A. georgei* - *Rubus amabilis* forest association). In the naming convention, a "-" was used to connect species from different layers, and "+" was to connect multiple species within the same layer (Guo et al., 2020).

4 Data description

4.1 Species composition

The HDM-Plot dataset compiles 14,113 individual records from 314 plots, documenting 1,127 plant species (including subspecies and varieties) belonging to 379 genera and 117 families (Table 1). The most species rich families are Rosaceae (133 species), Ericaceae (93), Fabaceae (66), Asteraceae (63), and Fagaceae (37), occurring in 27.1% to 71.3% of plots (Fig. 3; Table 2). These families show distinct spatial and elevational patterns (Fig. 3). Rosaceae and Fabaceae are widespread, whereas Ericaceae and Fagaceae are less frequent toward the northern sector and Asteraceae is reduced in the southernmost part. Along the ranges of elevation, Fabaceae spans the full gradient (750–5000 m). Rosaceae and Asteraceae extend to the highest elevations but generally occur above 1,100 and 1,700 m, respectively. Ericaceae is largely distributed in middle and high elevations (1,400–4,800 m), and Fagaceae extends from the lowest elevations up to 4,200 m. The five richest genera were *Rhododendron* (75 species), *Berberis* (34), *Cotoneaster* (30), *Salix* (24), and *Quercus* (22) (Table 2). *Rhododendron*, *Berberis*, and *Cotoneaster* are broadly distributed, while *Salix* is less in the central to southern HDM and *Quercus* is less toward the north. The dominant genera occupy wide elevational ranges of approximately 2,600–3,000 m, but their elevational lower and upper limits differ (Fig. 3).

Table 2 Composition of dominant plant families and genera in the HDM-Plot dataset

https://doi.org/10.5194/essd-2026-204
Preprint. Discussion started: 1 April 2026
© Author(s) 2026. CC BY 4.0 License.

Open Access Earth System Science Data Discussions

	Dominant families	Dominant genera
All	Rosaceae (133, 11.8%)	*Rhododendron* (75, 6.7%)
	Ericaceae (93, 8.3%)	*Berberis* (34, 3.0%)
	Fabaceae (66, 5.9%)	*Cotoneaster* (30, 2.7%)
	Asteraceae (63, 5.6%)	*Salix* (24, 2.1%)
	Fagaceae (37, 3.3%)	*Quercus* (22, 2.0%)
Forest	Rosaceae (99, 13.4%)	*Rhododendron* (61, 8.3%)
	Ericaceae (78, 10.6%)	*Berberis* (30, 4.1%)
	Fabaceae & Fagaceae (34, 4.6%)	*Cotoneaster* (23, 3.1%)
	Berberidaceae (30, 4.1%)	*Quercus* (20, 2.7%)
	Pinaceae (28, 3.8%)	*Salix* (19, 2.6%)
Shrubland	Rosaceae (58, 18.1%)	*Rhododendron* (33, 10.3%)
	Ericaceae (38, 11.8%)	*Cotoneaster* (19, 5.9%)
	Fabaceae (25, 7.8%)	*Berberis* (16, 5.0%)
	Berberidaceae (17, 5.3%)	*Salix* (12, 3.7%)
	Lamiaceae (14, 4.4%)	*Lonicera* (11, 3.4%)
Grassland	Asteraceae (52, 19.5%)	*Gentiana* (18, 6.8%)
	Cyperaceae & Ranunculaceae (24, 9.0%)	*Kobresia* & *Saussurea* (12, 4.5%)
	Gentianaceae (19, 7.1%)	*Anaphalis* (10, 3.8%)
	Fabaceae & Rosaceae (18, 6.8%)	*Artemisia* (9, 3.4%)
	Poaceae (17, 6.4%)	*Anemone* & *Carex* (8, 3.0%)

Dominant families and genera refer to the top five taxa ranked by number of species. An ampersand (&) connects families or genera with the same number of species. The values in parentheses indicate the number of species and its proportion of the total number of species in the corresponding category.

https://doi.org/10.5194/essd-2026-204
Preprint. Discussion started: 1 April 2026
© Author(s) 2026. CC BY 4.0 License.

Open Access Earth System Science Data Discussions

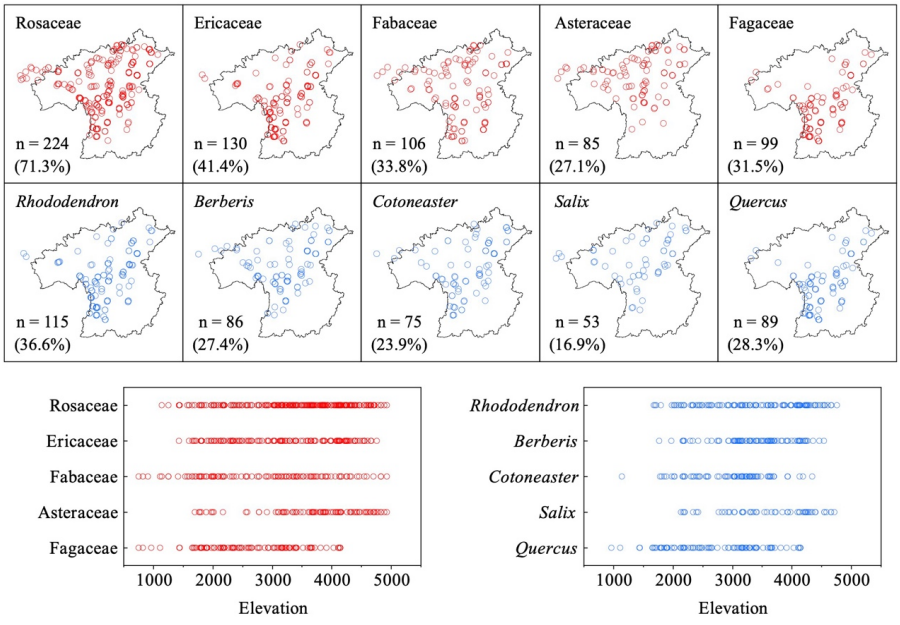

Figure 3. Spatial patterns of dominant plant families and genera in the HDM-Plot dataset. n denotes the number of plots in which dominant families and genera were recorded (the proportion of the total number of survey plots).

Taxonomic composition differs among vegetation types (Table 2; Fig. 4–6). Forest plots include 737 species, 238 genera, and 91 families (Table 1). The dominant families are Rosaceae, Ericaceae, Fabaceae, Fagaceae, Berberidaceae, and Salicaceae (Table 2). Rosaceae is mainly represented by shrub genera such as *Cotoneaster* (23.2%), *Rubus* (13.1%), and *Rosa* (12.1%), as well as tree genera such as *Prunus* (14.1%). Ericaceae is dominated by *Rhododendron* (78.2%), which is commonly shrubs and occasionally small trees. Fabaceae contains a wide range of growth form, including shrub genera (e.g., *Indigofera*, *Campylotropis*, and *Caragana*), climbers (mostly single-species genera), and occasional tree taxa (e.g., *Dalbergia*). Fagaceae is composed of *Quercus* (58.8%), *Lithocarpus* (20.6%), and *Castanopsis* (20.6%), and provides constructive species in nearly one-third of forest plots. Berberidaceae only records one genus *Berberis* and is a vital component of the shrub layer. Pinaceae offers the main needleleaf constructive species in needleleaf forests and mixed forests, dominated by *Abies* (35.7%), *Picea* (28.6%), *Larix* (10.7%), and *Pinus* (10.7%). Rosaceae and Pinaceae are

https://doi.org/10.5194/essd-2026-204
Preprint. Discussion started: 1 April 2026
© Author(s) 2026. CC BY 4.0 License.

Open Access Earth System Science Data Discussions

the most widely distributed families, and other four dominant families are concentrated in the southern HDM (Fig. 4). Fabaceae and Fagaceae show the lowest elevational lower limits, with upper limits close to 3,800 m and 4,100 m, respectively. Rosaceae, Ericaceae, and Pinaceae reach the highest upper limits (4,300 m), with lower limits between 1,300 and 1,500 m. Berberidaceae exhibits the narrowest elevational range (2,200–4,200 m). The top five genera are *Rhododendron*, *Berberis*, *Cotoneaster*, *Quercus*, and *Salix* (Table 2). The first four genera are restricted to the southern HDM, while *Salix* is more frequently recorded in the northern HDM (Fig. 4). The upper elevational limits of these genera are similar (4,100–4,300 m), whereas their lower limits differ. *Quercus* occurs down to 1,000 m, *Rhododendron* to 1,700 m, *Cotoneaster* to 1,800 m, and *Berberis* and *Salix* to approximately 2,100 m (Fig. 4).

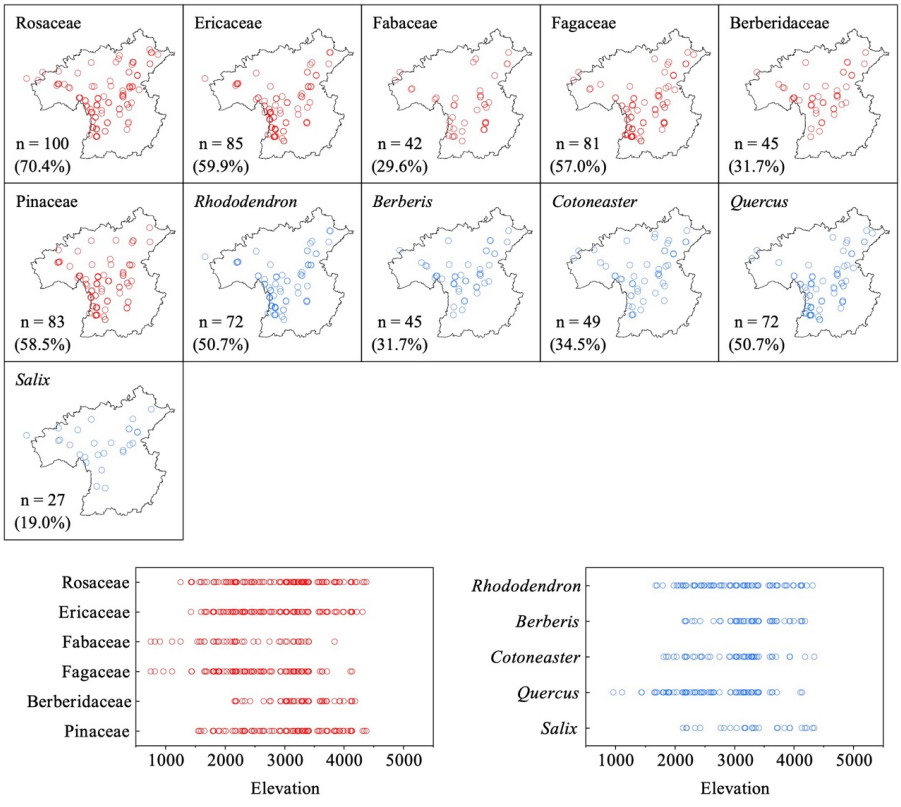

Figure 4. Spatial patterns of dominant plant families and genera in forest vegetation in the HDM-Plot dataset.

110 shrubland plots survey a total of 321 species from 124 genera and 53 families

https://doi.org/10.5194/essd-2026-204
Preprint. Discussion started: 1 April 2026
© Author(s) 2026. CC BY 4.0 License.

(Table 1). Dominant families largely overlap with those of forests, with Lamiaceae as a new component. Rosaceae consists of *Cotoneaster* (32.8%), *Rosa* (15.5%), and *Spiraea* (13.8%) and forms the core of deciduous broadleaf shrublands. Ericaceae is strongly dominated by *Rhododendron* (86.8%) and typically acts as the constructive species in evergreen broadleaf shrublands. Fabaceae includes *Caragana* (20.0%), *Campylotropis* (16.0%), and *Indigofera* (16.0%), commonly recorded in the dry-hot valley shrublands. Berberidaceae is almost represented by *Berberis* (94.1%), with *Mahonia* recorded but not in forest plots. Lamiaceae is characterized by typical dry-hot valley genera such as *Caryopteris* (28.6%), *Isodon* (21.4%), and *Elsholtzia* (21.4%). Rosaceae and Fabaceae are widespread, whereas Berberidaceae, Ericaceae, and Lamiaceae are heterogeneous in distribution (Fig. 5). Shrubland composition transitions from lower-elevational dry-hot valley components to middle and high elevations with increased representation of Ericaceae and Berberidaceae (Fig. 5). The top genera are *Rhododendron*, *Cotoneaster*, *Berberis*, *Salix*, and *Lonicera* (Table 2). *Berberis* and *Lonicera* are widely distributed across the region, whereas *Rhododendron*, *Cotoneaster*, and *Salix* are primarily aligned along a southwest–northeast direction. Although these genera occasionally occur at low elevations, they are largely distributed between 3,000 and 4,700 m, with *Cotoneaster* having the lowest upper limit (3,700 m) (Fig. 5).

https://doi.org/10.5194/essd-2026-204
Preprint. Discussion started: 1 April 2026
© Author(s) 2026. CC BY 4.0 License.

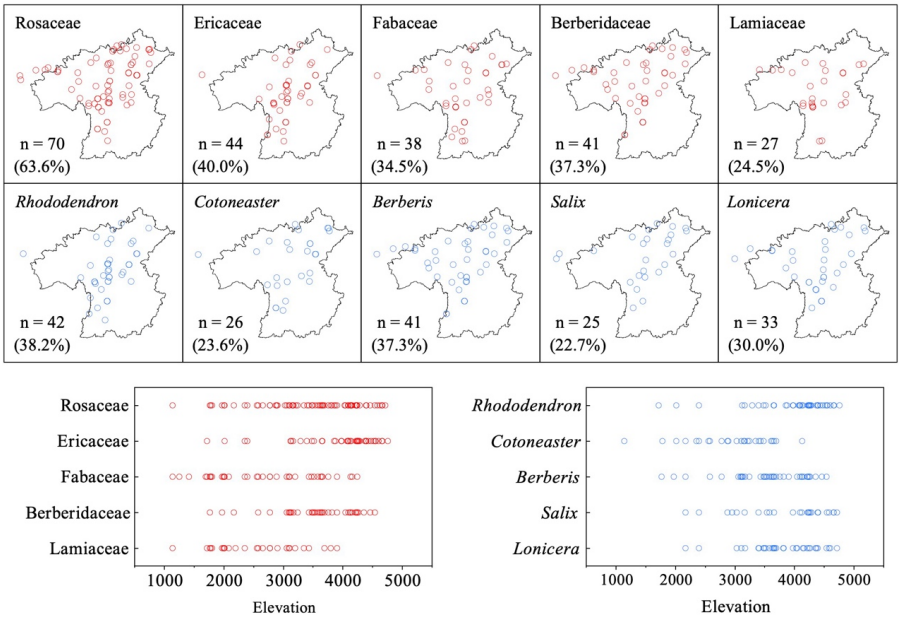

Figure 5. Spatial patterns of dominant plant families and genera in shrubland vegetation in the HDM-Plot dataset.

62 grassland plots investigate a total of 266 species belonging to 38 families and 113 genera (Table 1). The most species-rich families are Asteraceae, Cyperaceae, Ranunculaceae, Gentianaceae, Fabaceae, Rosaceae, and Poaceae (Table 2). Asteraceae is largely represented by *Saussurea* (23.1%), *Anaphalis* (19.2%), *Artemisia* (17.3%), and *Taraxacum* (13.5%), consisting of perennial forbs and semi-shrubs that contribute to forb grasslands. Cyperaceae is dominated by tussock *Kobresia* and rhizome *Carex* and provide the main constructive species in grassland vegetation (42 plots), especially the zonal species *K. pygmaea*. Ranunculaceae is represented by *Anemone* (33.3%) and *Ranunculus* (20.8%), Gentianaceae is strongly dominated by *Gentiana* (94.7%), and Fabaceae is composed of *Astragalus* (33.3%) and *Oxytropis* (27.8%). Rosaceae consists of perennial herbs such as *Argentina* (33.3%) and *Potentilla* (22.2%) and dwarf shrub *Dasiphora* (11.1%). Poaceae is dominated by tussock grasses, including *Poa* (17.6%), *Aristida* (17.6%), *Stipa* (11.8%), and *Festuca* (11.8%). Grassland families show broadly similar distributions across the surveyed region (Fig. 6). The dominant genera include *Gentiana*, *Kobresia*, *Saussurea*, *Anaphalis*, *Artemisia*, *Anemone*, and *Carex* (Table 2).

https://doi.org/10.5194/essd-2026-204
Preprint. Discussion started: 1 April 2026
© Author(s) 2026. CC BY 4.0 License.

Kobresia shows the broad distribution across both geographic space and the elevational gradient, whereas the other dominant genera exhibit distinct differentiation along both dimensions (Fig. 6).

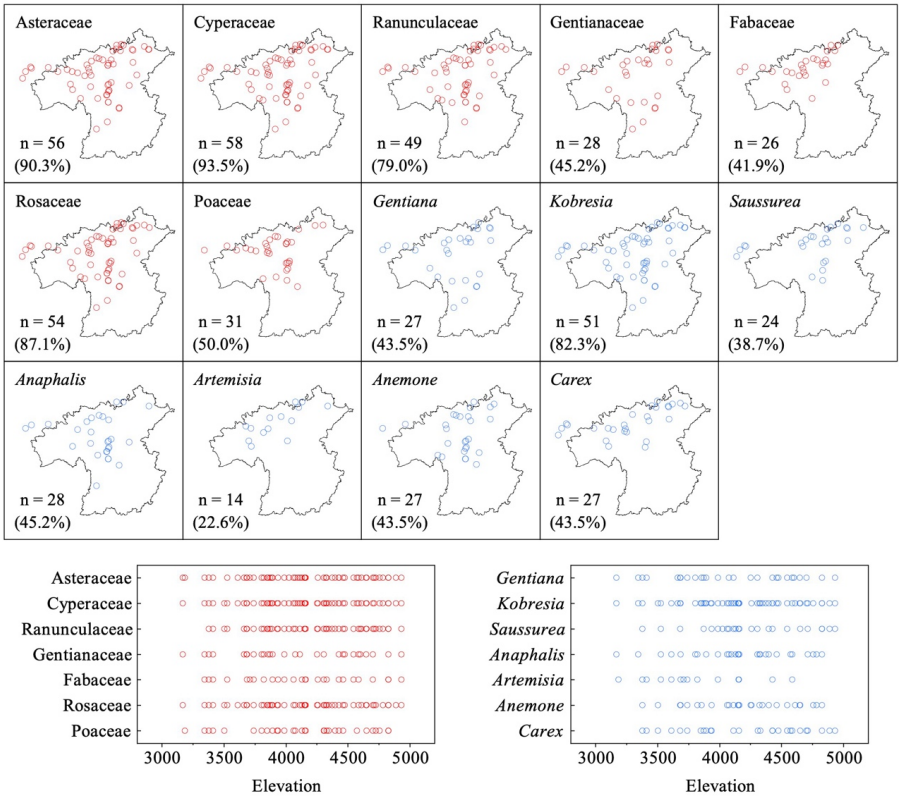

Figure 6. Spatial patterns of dominant plant families and genera in grassland vegetation in the HDM-Plot dataset.

4.2 Growth forms and life forms

The 1,127 species in the HDM-Plot dataset can be categized into five growth forms. Shrubs comprise the largest proportion of recorded species (46.0%), followed by trees (27.3%) and herbs (23.6%), while climbers (2.0%) and semi-shrubs (1.2%) contribute a small number of species (Fig. 7). Among herbs, perennials dominate (92.1%), and annuals (6.0%) and biennials (1.9%) are comparatively rare. Woody species show clear contrasts in leaf type and phenology. Shrubs are almost composed of broadleaf (98.7%), with deciduous shrubs (59.7%) more frequent than evergreen shrubs (40.4%), whereas trees exhibit a higher proportion of needleleaf species (11.7%) and a near balance

https://doi.org/10.5194/essd-2026-204
Preprint. Discussion started: 1 April 2026
© Author(s) 2026. CC BY 4.0 License.

between evergreen (52.3%) and deciduous (47.8%) species (Fig. 7).

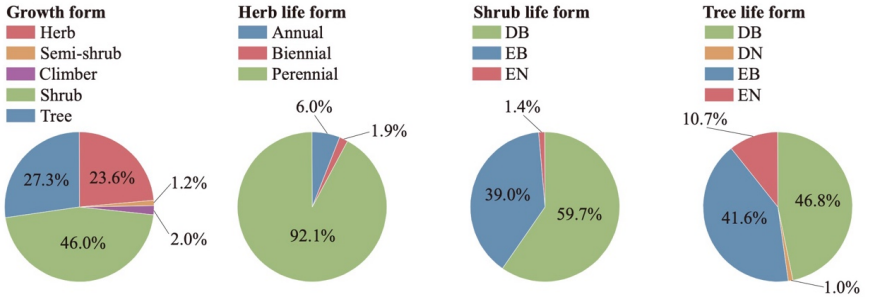

Figure 7. Growth forms and life forms of plant species surveyed in the HDM-Plot dataset. DB, deciduous broadleaf; DN, deciduous needleleaf; EB, evergreen broadleaf; EN, evergreen needleleaf. Pie charts show life form classifications for dominant herbs, shrubs, and trees only, and detailed life form information for all species is provided in the species list of the published dataset.

Pooled species richness along the elevational gradient shows a unimodal pattern at the regional scale (Fig. 8), increasing from low elevations to a maximum at 3,000–4,000 m and then declining sharply. Four individual mountains with broad elevational coverage (Gaoligong Mt; Nushan Mt; Daxue Mt; and Minshan Mt; Fig. 2) show similar unimodal patterns, although peak richness occurs at 2,000–3,000 m in these mountains (Fig. 8).

Growth form composition varies significantly with elevation (Fig. 8). The relative contribution of trees is highest at low elevations and declines with increasing elevation, shrubs remain important across all belts and peak at middle elevations (2,000–3,000 m), and herbs increase strongly toward high elevations. Woody life form composition also shifts with elevation (Fig. 8). For shrubs, evergreen broadleaf shrubs are most frequent in low elevations (0–1,000 m), deciduous broadleaf shrubs dominate from middle to high elevations (1,000–5,000 m), and evergreen needleleaf shrubs occur mainly above 2,000 m. Life form composition of trees shows more significant elevational shifts. Evergreen broadleaf trees are common at low elevations but decrease with elevation, deciduous broadleaf trees increase to middle elevations and then decline, evergreen needleleaf trees rise rapidly above 1,000 m and dominate at high elevations, and deciduous needleleaf trees are largely restricted to the high-elevational belt (3,000–5,000 m) (Fig. 8). At the mountain scale, several elevational trends are consistent with

https://doi.org/10.5194/essd-2026-204
Preprint. Discussion started: 1 April 2026
© Author(s) 2026. CC BY 4.0 License.

the regional pattern, but changes specific to individual mountains are also evident and unique (Fig. 8).

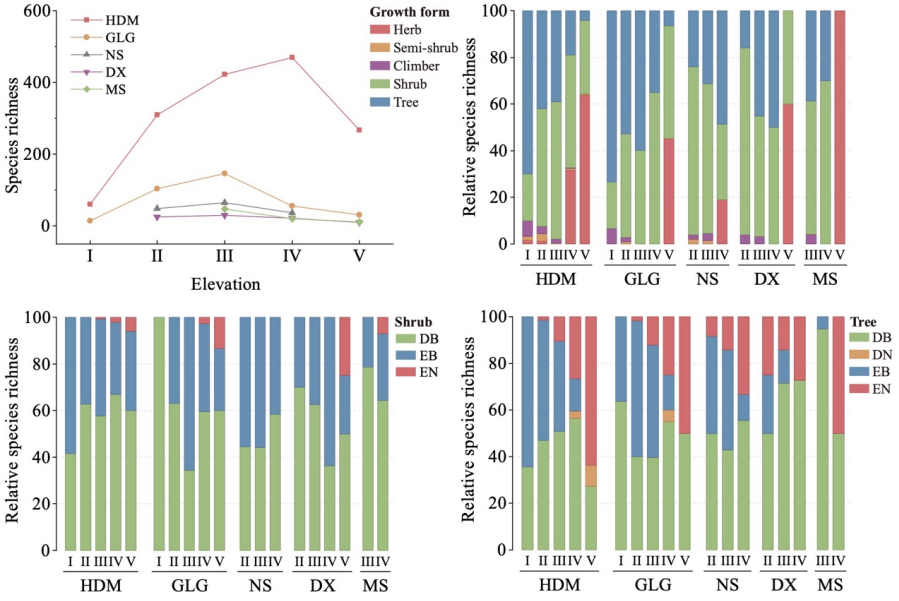

Figure 8. Changes in species richness of growth forms and life forms along elevational gradients in the HDM-Plot dataset. Elevational patterns are summarized at two scales. Regional scale (HDM, Hengduan Mountains): species richness represents the combined number of unique species with each elevational belt across the entire study area. Elevational belts are defined as I, 0–1000 m; II,1000–2000 m; III, 2000–3000 m; IV, 3000–4000 m; and V, 4000–5000 m. Local scale: four representative mountains with extensive elevational gradients distributed from south to north within the dataset are selected. GLG, Gaoligong Mountain; NS, Nushan Mountain; DX, Daxue Mountain; and MS, Minshan Mountain. The abbreviations of woody life forms are defined as follows: DB, deciduous broadleaf; DN, deciduous needleleaf; EB, evergreen broadleaf; EN, evergreen needleleaf.

4.3 Floristic characteristics

At the family level, 117 families can be assigned to 10 areal-type categories (Fig. 9). Cosmopolitan families account for 30.8% of the total, tropical families for 39.3%, and temperate families for 29.9%. Pantropic families comprise the largest share within tropical families (63.0%), with species-rich families including Lauraceae, Sapindaceae, Celastraceae, Euphorbiaceae, and Anacardiaceae. North temperate families account for 62.9% of the temperate component, represented by Ericaceae, Fagaceae, Berberidaceae, Salicaceae, and Pinaceae. These patterns reflect that the floristic composition of the HDM retains a tropical–subtropical elements and also incorporating temperate–alpine

https://doi.org/10.5194/essd-2026-204
Preprint. Discussion started: 1 April 2026
© Author(s) 2026. CC BY 4.0 License.

attributes.

At the genus level, 379 genera can be assigned into 15 areal-type categories (Fig. 9). Temperate genera dominate (54.1%), followed by tropical genera (35.4%), whereas cosmopolitan (6.6%) and Chinese endemic genera (4.0%) are less frequent. Temperate genera are mainly north temperate (42.9%), represented by *Rhododendron*, *Berberis*, *Cotoneaster*, *Salix*, and *Quercus*. For tropical genera, pantropical (32.8%) and tropical Asian (28.4%) areal-types are most common, with *Ilex* and *Indigofera* as pantropical representatives and *Fargesia*, *Leptodermis*, *Caryopteris*, and *Corylopsis* as East Asian representatives. Compared with the family level, the genus level composition shows a clear shift toward temperate elements.

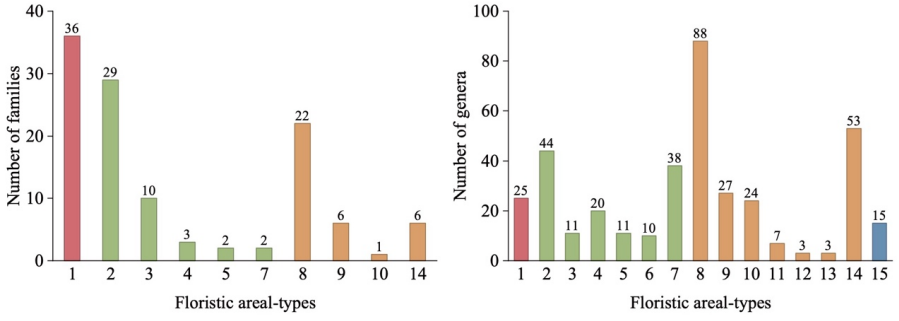

Figure 9. Floristic areal-types of plant families and genera surveyed in the HDM-Plot dataset. 1, Cosmopolitan; 2, Pantropic; 3, Tropical Asia & Tropical America disjuncted; 4, Old World Tropics; 5, Tropical Asia & Tropical Australasia; 6, Tropical Asia to Tropical Africa; 7, Tropical Asia (Indo–Malaysia); 8, North Temperate; 9, East Asia & North America disjuncted; 10, Old World Temperate ; 11, Temperate Asia; 12, Mediterranean, West Asia to Central Asia; 13, Central Asia; 14, East Asia; 15, Endemic to China (Wu, 1991, 1993). The green and orange bars represent tropical and temperate areal-types, respectively, whereas the red and blue bars reflect cosmopolitan and endemic to China areal-types, respectively.

4.4 Vegetation classification

Based on field surveys and the *revised vegetation classification system of China* (Guo et al., 2020), 314 plots can be classified into three vegetation formation groups, namely forest, shrubland, and grassland (Fig. 10–11; Table 3). These plots can be further classified into 18 vegetation formations, 142 alliance groups, 209 alliances, 238 association groups, and 299 associations.

https://doi.org/10.5194/essd-2026-204
Preprint. Discussion started: 1 April 2026
© Author(s) 2026. CC BY 4.0 License.

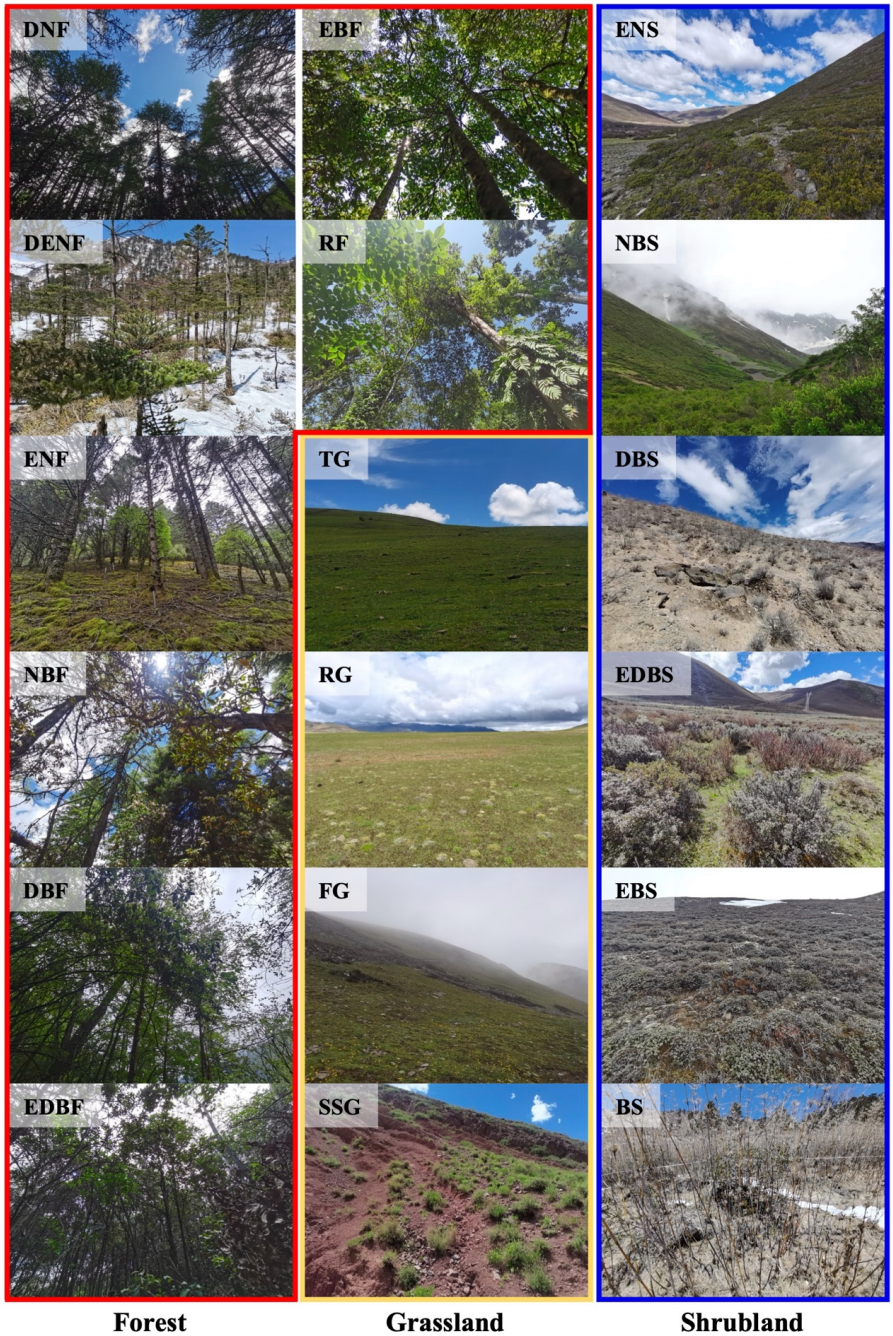

Figure 10. Plot photos across 18 vegetation formations in the HDM-Plot dataset. DNF, deciduous needleleaf forest; DENF, mixed deciduous and evergreen needleleaf forest; ENF, evergreen needleleaf forest; NBF, mixed needleleaf and broadleaf forest; DBF, deciduous broadleaf forest; EDBF, mixed evergreen and deciduous broadleaf forest; EBF, evergreen broadleaf forest; RF,

https://doi.org/10.5194/essd-2026-204
Preprint. Discussion started: 1 April 2026
© Author(s) 2026. CC BY 4.0 License.

rainforest; ENS, evergreen needleleaf shrubland; NBS, needleleaf and broadleaf shrubland; DBS, deciduous broadleaf shrubland; EDBS, evergreen and deciduous broadleaf shrubland; EBS, evergreen broadleaf shrubland; BS, bamboo shrubland; TG, tussock grassland; RG, rhizome grassland; FG, forb grassland; SSG, semi-shrubby grassland.

Table 3 Vegetation classification of plant communities in the HDM-Plot dataset

Vegetation formation group	Vegetation formation	Alliance group	Number of Plot
Forest	DNF	*Larix*	4
	DENF	*Larix* + *Abies*	1
	ENF	*Abies*	12
		Cunninghamia	1
		Juniperus	3
		Picea	8
		Picea + *Juniperus*	1
		Pinus	21
		Tsuga	3
		Tsuga + *Abies*	1
	NBF	*Abies* + *Quercus*	3
		Abies + *Rhododendron*	1
		Abies + *Sorbus*	1
		Acer + *Cephalotaxus*	1
		Juniperus + *Salix*	1
		Picea + *Betula*	1
		Picea + *Quercus*	1
		Pinus + *Alnus*	3
		Pinus + *Castanopsis*	1
		Pinus + *Lithocarpus*	2
		Pinus + *Populus*	1
		Pinus + *Quercus*	2
		Taxus + *Acer*	1
		Tsuga + *Lithocarpus*	1
	DBF	*Alnus*	6
		Alnus + *Quercus*	1
		Betula	5
		Dalbergia	1
		Populus	3
		Populus + *Litsea* + *Viburnum*	1
		Prunus	2
		Pyrus	1
		Quercus	3
		Salix	2
		Tilia + *Cornus* + *Corylus*	1
		Toxicodendron + *Quercus*	1

https://doi.org/10.5194/essd-2026-204
Preprint. Discussion started: 1 April 2026
© Author(s) 2026. CC BY 4.0 License.

Open Access Earth System Science Data Discussions

	EDBF	*Alnus* + *Castanopsis*	1
		Alnus + *Saurauia*	1
		Alnus + *Ternstroemia*	1
		Betula + *Quercus*	1
		Castanopsis + *Litsea*	1
		Castanopsis + *Quercus*	1
		Pistacia + *Dalbergia*	1
		Quercus + *Albizia*	1
		Quercus + *Corylopsis*	1
		Quercus + *Pistacia*	1
		Salix + *Quercus*	1
	EBF	*Acacia*	1
		Castanopsis	1
		Exbucklandia + *Schima*	1
		Lithocarpus	1
		Lithocarpus + *Quercus* + *Symplocos*	1
		Mallotus + *Ficus*	1
		Mallotus + *Machilus*	1
		Morella	1
		Pistacia	2
		Quercus	12
		Quercus + *Ilex*	1
		Sarcosperma	1
		Saurauia	1
		Schima	1
	RF	*Aidia* + *Oreocnide*	1
		Altingia	1
		Castanopsis + *Altingia*	1
Shrubland	ENS	*Juniperus*	10
	NBS	*Juniperus* + *Ribes* + *Spiraea*	1
		Salix + *Juniperus*	1
		Sibiraea + *Juniperus* + *Caragana*	1
	DBS	*Abelia* + *Berberis* + *Rosa* + *Cotinus*	1
		Ajania	1
		Artemisia	1
		Berberis	6
		Berberis + *Cotoneaster*	1
		Berberis + *Lonicera*	1
		Caryopteris	2
		Corylus	1
		Cotoneaster - *Artemisia*	1
		Elsholtzia + *Rubus* + *Hypericum* + *Viburnum*	1
		Excoecaria	1
		Lonicera + *Cotoneaster*	1

https://doi.org/10.5194/essd-2026-204
Preprint. Discussion started: 1 April 2026
© Author(s) 2026. CC BY 4.0 License.

		Prunus + *Zanthoxylum* + *Isodon*	1
		Rhamnus	2
		Rosa	2
		Rosa + *Berberis* + *Isodon*	1
		Rosa + *Cotoneaster* + *Berberis*	1
		Salix	7
		Salix + *Dasiphora*	1
		Sibiraea	2
		Sibiraea + *Salix*	1
		Sophora	1
		Sophora + *Bauhinia*	1
		Sophora + *Leptodermis*	1
		Spiraea	1
		Vitex	1
	EDBS	*Ajania* + *Daphne*	1
		Campylotropis + *Daphne*	1
		Dasiphora + *Rhododendron*	1
		Flueggea + *Clematis*	1
		Isodon + *Rosa*	1
		Itea + *Viburnum* + *Bauhinia*	1
		Prinsepia + *Rosa*	1
		Quercus + *Olea* + *Pistacia* + *Excoecaria*	1
		Rhododendron + *Cotoneaster*	1
		Rhododendron + *Salix*	1
		Rhododendron + *Sorbus*	1
		Rosa + *Caryopteris* - *Artemisia*	1
		Zanthoxylum + *Chrysojasminum*	1
		Zanthoxylum + *Rhamnus*	1
	EBS	*Daphne* + *Quercus*	1
		Dodonaea	1
		Gaultheria	1
		Lithocarpus + *Castanopsis*	1
		Osteomeles + *Fargesia*	1
		Pistacia	1
		Quercus	12
		Rhododendron	22
	BS	*Fargesia*	2
Grassland	TG	*Carex*	1
		Carex + *Kobresia*	2
		Festuca	1
		Festuca + *Carex*	1
		Festuca+ *Kobresia*	1
		Kobresia	25
		Kobresia+ *Argentina*	1

https://doi.org/10.5194/essd-2026-204
Preprint. Discussion started: 1 April 2026
© Author(s) 2026. CC BY 4.0 License.

	Kobresia + *Potentilla*	1
	Poa	1
	Poa + *Bistorta*	1
RG	*Carex*	5
	Carex + *Kobresia*	2
	Carex + *Kobresia* + *Blysmus*	1
	Carex + *Potentilla*	1
	Carex + *Stipa*	1
	Trichophorum	1
FG	*Anaphalis*	1
	Anaphalis + *Argentina*	1
	Androsace	1
	Argentina	5
	Artemisia	1
	Bistorta	1
	Bistorta + *Trollius*	1
	Eremogone	1
	Salix - *Anemone*	1
	Sibbaldia	1
SSG	*Artemisia*	2

DNF, deciduous needleleaf forest; DENF, mixed deciduous and evergreen needleleaf forest; ENF, evergreen needleleaf forest; NBF, mixed needleleaf and broadleaf forest; DBF, deciduous broadleaf forest; EDBF, mixed evergreen and deciduous broadleaf forest; EBF, evergreen broadleaf forest; RF, rainforest; ENS, evergreen needleleaf shrubland; NBS, needleleaf and broadleaf shrubland; DBS, deciduous broadleaf shrubland; EDBS, evergreen and deciduous broadleaf shrubland; EBS, evergreen broadleaf shrubland; BS, bamboo shrubland; TG, tussock grassland; RG, rhizome grassland; FG, forb grassland; SSG, semi-shrubby grassland.

Forest vegetation formation group includes eight vegetation formations: deciduous needleleaf forest (DNF), mixed deciduous and evergreen needleleaf forest (DENF), evergreen needleleaf forest (ENF), mixed needleleaf and broadleaf forest (NBF), deciduous broadleaf forest (DBF), mixed evergreen and deciduous broadleaf forest (EDBF), evergreen broadleaf forest (EBF), and rainforest (RF) (Table 3). DNF includes only one alliance (*Larix potaninii* var. *macrocarpa*) and appears at 3,732–4,136 m in the central and northwestern HDM. DENF is also rare and was recorded from a single plot in Fugong (western border between China and Myanmar) at 3,247 m. ENF is widespread throughout the HDM at 1,809–4,377 m and is constructed by *Pinus*, *Abies*, *Picea*, *Juniperus*, and *Tsuga*. NBF is concentrated in the southern HDM at 1,801–4,189 m and typically combines *Pinus*, *Abies* and *Picea* with broadleaf trees such as *Quercus*,

https://doi.org/10.5194/essd-2026-204
Preprint. Discussion started: 1 April 2026
© Author(s) 2026. CC BY 4.0 License.


Alnus, and *Lithocarpus*. DBF is widely distributed at 1,256–4,217 m, excluding the northwestern HDM, and is commonly constructed by *Alnus*, *Betula*, *Quercus*, and *Populus*. EDBF occurs patchily from the southwestern to northeastern HDM at 966–3,298 m, where evergreen components mainly *Quercus* and *Castanopsis* co-occur with deciduous broadleaf taxa such as *Alnus*. EBF is widespread at low to middle elevations (906–3,636 m) and is most frequently constructed by *Quercus*. RF is restricted to the lowest elevations in Medog, southeastern corner of Tibet region (754–1,431m) and is characterized by tropical and subtropical trees (Fig. 11).

Shrubland vegetation formation group can be further divided into six vegetation formations: evergreen needleleaf shrubland (ENS), needleleaf and broadleaf shrubland (NBS), deciduous broadleaf shrubland (DBS), evergreen and deciduous broadleaf shrubland (EDBS), evergreen broadleaf shrubland (EBS), and bamboo shrubland (BS) (Table 3). ENS consists of two alliances (*Juniperus squamata* and *J. convallium*) and occurs mainly along the central and northwestern margin of the HDM at 3,757–4,668 m. NBS is rare and was surveyed from high-elevational area (4,044–4,720 m) in Chamdo, eastern Tibet, where *Juniperus* co-occurs with broadleaf shrubs including *Ribes*, *Salix*, and *Spiraea*. DBS is widespread across the HDM at 1,772–4,662 m and is most frequently dominated by *Berberis*, *Salix*, *Rosa*, *Cotoneaster*, and *Sibiraea*. EDBS spans a broad elevational gradient (1,144–4,226 m) from the central to northeastern HDM and features mixtures of evergreen (e.g., *Rhododendron* and *Daphne*) with deciduous components (e.g., *Rosa* and *Zanthoxylum*). EBS is widely distributed from the southwestern to northeastern HDM at 1,257–4,758 m and is commonly dominated by *Rhododendron* and *Quercus*. BS is uncommon in the dataset and was found in Yunnan Province at 3,120–3,290 m and includes two alliances (*Fargesia gongshanensis* and *F. melanostachys*) (Fig. 11).

Grassland vegetation formation group comprises four vegetation formations: tussock grassland (TG), rhizome grassland (RG), forb grassland (FG), and semi-shrub grassland (SSG) (Table 3). TG is widespread across the HDM at 3,168–4,932 m and is strongly dominated by *Kobresia*, especially the widespread alpine meadow species *K. pygmaea* (24 plots). RG occurs mainly in the northern HDM at 3,379–4,701 m and is

https://doi.org/10.5194/essd-2026-204
Preprint. Discussion started: 1 April 2026
© Author(s) 2026. CC BY 4.0 License.

480 represented by *Carex*, with *C. enervis* frequently recorded. FG is concentrated from the
481 central to northern HDM at 3,345–4,784 m and is characterized by forb constructed
482 communities, with *Argentina* as a common genus. SSG is rare and has a single alliance
483 (*Artemisia vestita*), observed in dry-hot valleys in the northwestern HDM at 3,186–
484 3,710 m (Fig. 11).

https://doi.org/10.5194/essd-2026-204
Preprint. Discussion started: 1 April 2026
© Author(s) 2026. CC BY 4.0 License.

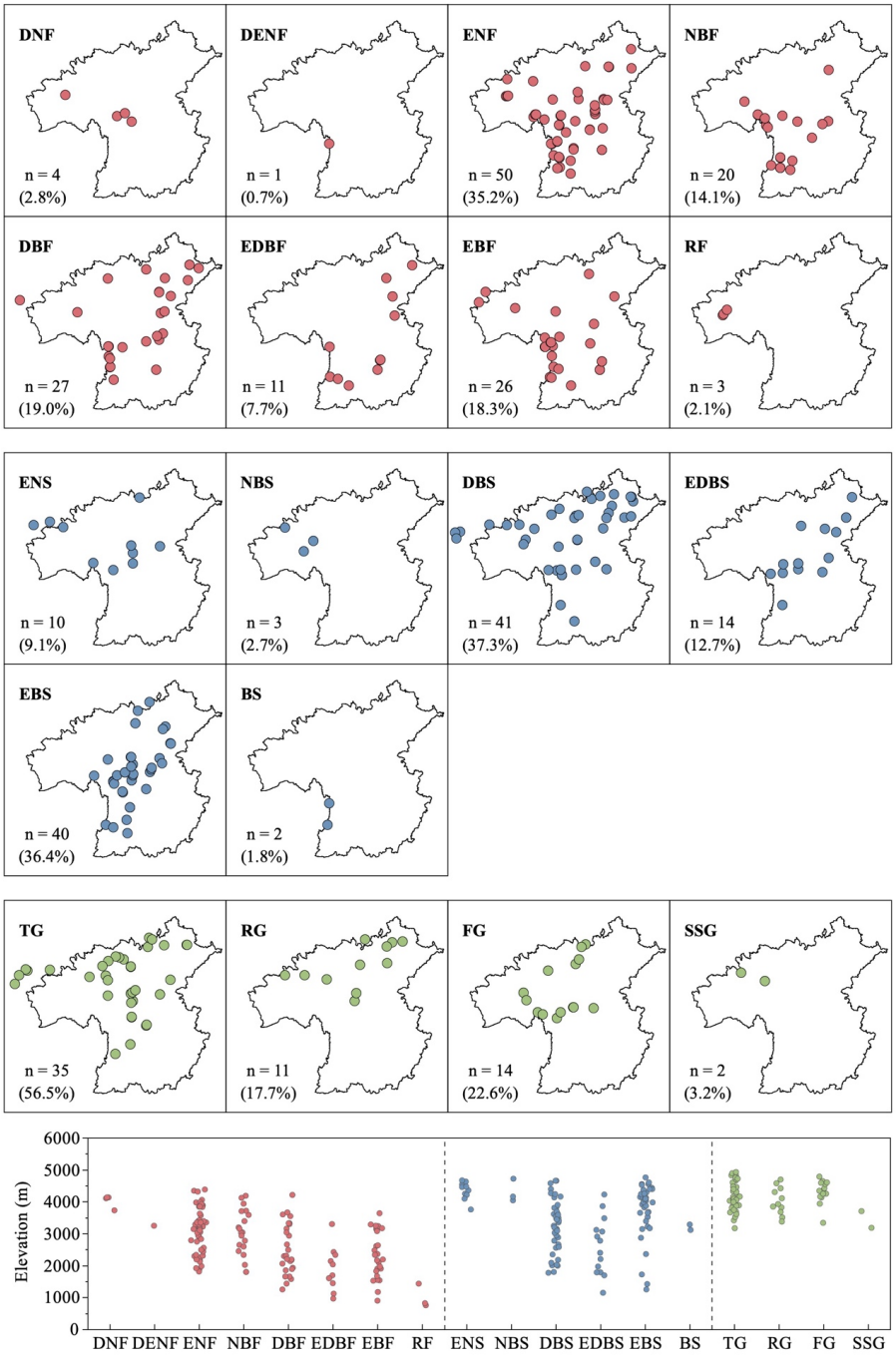

Figure 11. Horizontal and elevational distribution of vegetation in the HDM-Plot dataset. Red, blue, and green dots represent forest, shrubland, and grassland vegetation formation group, respectively. DNF, deciduous needleleaf forest; DENF, mixed deciduous and evergreen needleleaf forest; ENF,

https://doi.org/10.5194/essd-2026-204
Preprint. Discussion started: 1 April 2026
© Author(s) 2026. CC BY 4.0 License.

evergreen needleleaf forest; NBF, mixed needleleaf and broadleaf forest; DBF, deciduous broadleaf forest; EDBF, mixed evergreen and deciduous broadleaf forest; EBF, evergreen broadleaf forest; RF, rainforest; ENS, evergreen needleleaf shrubland; NBS, needleleaf and broadleaf shrubland; DBS, deciduous broadleaf shrubland; EDBS, evergreen and deciduous broadleaf shrubland; EBS, evergreen broadleaf shrubland; BS, bamboo shrubland; TG, tussock grassland; RG, rhizome grassland; FG, forb grassland; SSG, semi-shrubby grassland.

5 Data availability

The HDM-Plot dataset includes two components: a plot dataset and a habitat photo dataset. The plot dataset is provided as a Microsoft Excel format containing six sheets: 1) summary (Table 4); 2) basic plot information; 3) raw plot survey data; 4) species list; 5) species important values; and 6) vegetation classification. The habitat photo dataset is organized by survey period (i.e., 202203, 202205, 2023, and 2024). Photo files are provided in JPG format, named by plot ID, and correspond to the plots in the dataset. The dataset is publicly available through the National Tibetan Plateau / Third Pole Environment Data Center (Jin et al., 2026; https://doi.org/10.11888/Terre.tpdc.303394).

Table 4 Summary information of the HDM-Plot dataset.

Heading	Description	Type
Plot No	Plot number based on survey time	Code
Province	Administrative province of the plot location	Character
Longitude (°E)	Longitude in decimal degrees by GPS	Numeric
Latitude (°N)	Latitude in decimal degrees by GPS	Numeric
Elevation (m)	Elevation in decimal degrees by GPS	Integer
Disturbance intensity	Degree of disturbance recorded in the survey	Character
Plot size (m × m)	Plot size = plot length × plot width	Character
Community height (m)	Maximum plant height in the plot	Numeric
Community coverage (%)	Total vegetation coverage of the plot	Integer
Species richness	Number of species recorded in the plot	Integer
Latin name	Scientific name of the species (Flora of China, FOC)	Character
Growth form	Tree, shrub, climber, semi-shrub, and herb	Character
Phenological period	Phenological stage during survey (e.g., leaf period)	Character

https://doi.org/10.5194/essd-2026-204
Preprint. Discussion started: 1 April 2026
© Author(s) 2026. CC BY 4.0 License.

Number of plants (clusters)	Number of individuals or clumps recorded	Integer
Height (m)	Leaf-layer height (herb) / canopy height (woody)	Numeric
FBH (cm)	Reproductive branch height (herb)	Numeric
BD (cm)	Base diameter	Numeric
DBH (cm)	Diameter at breast height	Numeric
Crown a (m)	Maximum crown width (woody)	Numeric
Crown b (m)	Crown width perpendicular to maximum axis (woody)	Numeric
Coverage (%)	Specific species coverage (herb)	Numeric
Plant status	Vitality status of the individual (e.g., dead wood)	Character
Chinese name	Chinese name of the species (FOC)	Character
Genus	Genus of the species (FOC)	Character
Family	Family of the species (FOC)	Character
Leaf phenology	Deciduous vs. Evergreen	Character
Leaf type	Broadleaf vs. needleleaf	Character
Life span	Annual, biennial, and perennial	Character
No. of plots observed	Number of plots in which the species was recorded	Integer
Layer	Vegetation layer (e.g., tree layer)	Character
IV (%)	Importance value of the species within the plot	Numeric
Vegetation formation group	Supplementary upper-level unit (e.g., forest)	Character
Vegetation formation	Upper-level unit (e.g., evergreen needleleaf forest)	Character
Alliance group	Supplementary middle-level unit (e.g., *Abie* forest)	Character
Alliance	Middle-level unit (e.g., *A. georgei* forest)	Character
Association group	Supplementary lower-level unit (e.g., *A. georgei* - shrub forest)	Character
Association	Lower-level unit (*A. georgei* - *Rubus amabilis* forest)	Character

6 Summary

The HDM-Plot dataset was compiled from four extensive fieldworks conducted by our research group between 2022 and 2024. It provides detailed raw records from

https://doi.org/10.5194/essd-2026-204
Preprint. Discussion started: 1 April 2026
© Author(s) 2026. CC BY 4.0 License.

314 vegetation plots spanning major vegetation types in the HDM, from low-elevational dry-hot valleys to subalpine and alpine areas. The dataset offers a robust, standardized data for studies of vegetation ecology, conservation planning, and ecological restoration in this biodiversity hotspot, and provides an important regional complement to global vegetation plot compilations such as sPlot (Sabatini et al., 2021).

Several limitations remain due to the challenging field conditions and constraints in manpower and resources. First, the HDM have extremely complex topography and highly heterogeneous vegetation, and steep terrain often prevented the establishment of fully standardized plots. As a result, plot size could not always be kept uniform, and plot distribution may be uneven in some areas, which can affect representativeness and comparability. Second, given the high diversity and strong spatial turnover of species composition, individual plots may not fully capture the regional variability, potentially producing sampling bias. Third, some plot attributes, such as plant height, crown width, and coverage, were visually estimated in the field and may therefore be subject to observer uncertainty. Nevertheless, assembling a large, structurally detailed plot dataset under harsh field conditions represents a vital contribution, and we expect the HDM-Plot dataset to provide a valuable reference for ongoing and future efforts of vegetation reassessment and ecological research across the region.

Compared with our previously published dataset on the Tibetan Plateau (Jin et al., 2022), the HDM-Plot dataset fills a key geographic gap on the southeastern Plateau and demonstrates enhanced representativeness about plot distribution, species richness, and vegetation types. Plots are not restricted to areas along major roads, but also extend into accessible valleys and pathways. This is the first comprehensive vegetation plot dataset for the HDM to our knowledge with broad spatial coverage and representation of diverse vegetation types. In addition to raw species composition records, the dataset provides standardized geographic coordinates, species list, and hierarchical vegetation classifications.

During vegetation classification, we observed shrubland communities in which co-constructive species differ in leaf type and phenology, analogous to mixed forests. For example, shrublands jointly dominated by *Juniperus* and *Rhododendron* combine

https://doi.org/10.5194/essd-2026-204
Preprint. Discussion started: 1 April 2026
© Author(s) 2026. CC BY 4.0 License.

needleleaf and broadleaf components and may include evergreen and deciduous elements. Accordingly, we introduced two shrubland vegetation formations within the Guo et al. (2020) scheme: (a) needleleaf and broadleaf shrubland, and (b) evergreen and deciduous broadleaf shrubland. Similarly, in grasslands, co-constructive species often belong to different functional groups (e.g., tussock, rhizome, and forb), which are not always clearly separated in the current classification framework. We therefore retained multiple co-constructive species in alliance naming, while identifying the vegetation formation according to the life form of the species with the highest IV. For example, *Kobresia pygmaea* + *Potentilla saundersiana* grassland alliance was classified as a tussock grassland vegetation formation. These plot-based findings and standardized data provide support for the ongoing revision of China's vegetation classification system (Guo et al., 2020) and for the update of *Vegegraphy of China* (Fang et al., 2020). The ecological environment of southwestern China is highly fragile and increasingly exposed to human pressures, with limited capacity for natural recovery. Updated and standardized baseline data is therefore essential for guiding conservation, ecological planning, and restoration strategies, and for supporting biodiversity assessments and ecosystem management in this global hotspot under ongoing and future climate change.

Author contributions. JN conceived the study. JN and XM led the field works. YJ, LY, CY, XH, HX, YH, KW, and SS participated in vegetation survey. SS processed the climate maps. YJ and LY processed the dataset, performed the analyses and wrote the first draft. JN, XM and YJ improved the manuscript. All the authors approved the final version of the submitted manuscript.

Competing interests. The (co-) authors declare that they have no conflict of interest.

Disclaimer. Publisher's note: Copernicus Publications remains neutral with regard to jurisdictional claims in published maps and institutional affiliations.

Acknowledgements. The authors sincerely thank Qiuting Chen, Tingting Chen, Zhichao Chen, Tao Fang, Chuting Hu, Saijing Liu, Xiaoling Lu, Chenling Wang, Haoyan Wang, Jie Xia, Yang Yang, Pingqian Ye, Bohan Zheng, Yawen Zheng, and Yan Zhou from Zhejiang Normal University for their help in the field survey, Dashan He from Sichuan University for helping with specimen identification, and Ke Guo from

https://doi.org/10.5194/essd-2026-204
Preprint. Discussion started: 1 April 2026
© Author(s) 2026. CC BY 4.0 License.

Institute of Botany, the Chinese Academy of Sciences for providing assistance in vegetation classification.

Financial support. This work was supported by the Second Tibetan Plateau Scientific Expedition and Research Program (grant no. 2019QZKK0402).

References

Chi, X. F., Zhang, F. Q., Gao, Q. B., Xing, R., and Chen, S. L.: Genetic structure and eco-geographical differentiation of *Lancea tibetica* in the Qinghai-Tibetan Plateau, Genes, 10, 97, https://doi.org/10.3390/genes10020097, 2019.

Ding, W. N., Ree, R. H., Spicer, R. A., and Xing, Y. W.: Ancient orogenic and monsoon-driven assembly of the world's richest temperate alpine flora, Science, 369, 578–581, https://doi.org/10.1126/science.abb4484, 2020.

Editorial Committee of the Flora of China: Reipublicae Popularis Sinicae, 80 volumes, Science Press, Beijing, 1959–2004.

Editorial Committee of Vegetation of China: Vegetation of China, Science Press, Beijing, 1980.

Editorial Committee of Vegetation Map of China, Chinese Academy of Sciences: Vegetation of China and Its Geographical Pattern – Illustration of the Vegetation Map of the People's Republic of China (1:1,000,000), Geology Press, Beijing, 2007a.

Editorial Committee of Vegetation Map of China, Chinese Academy of Sciences: Vegetation Map of the People's Republic of China (1:1,000,000), Geology Press, Beijing, 2007b.

Fang, J. Y., Wang, X. P., Shen, Z. H., Tang, Z. Y., He, J. S., Yu, D., Jiang, Y., Wang, Z. H., Zheng, C. Y., Zhu, J. L., and Guo, Z. D.: Methods and protocols for plant community inventory, Biodiv. Sci., 17, 533–548, https://doi.org/10.3724/SP.J.1003.2009.09253, 2009.

Fang, J. Y., Guo, K., Wang, G. H., Tang, Z. Y., Xie, Z. Q., Shen, Z. H., Wang, R. Q., Qiang, S., Liang, C. Z., Da, L. J., and Yu, D.: Vegetation classification system and classification of vegetation types used for the compilation of vegetation of China, Chin. J. Plant Ecol., 44, 96–110, 2020.

Farr, T. G., Rosen, P. A., Caro, E., Crippen, R., Duren, R., Hensley, S., Kobrick, M., Paller, M., Rodriguez, E., Roth, L., Seal, D., Shaffer, S., Shimada, J., Umland, J., Werner, M., Oskin, M., Burbank, D., and Alsdorf, D.: The Shuttle Radar Topography Mission, Rev. Geophys., 45: RG2004, https://doi.org/10.1029/2005RG000183, 2007.

https://doi.org/10.5194/essd-2026-204
Preprint. Discussion started: 1 April 2026
© Author(s) 2026. CC BY 4.0 License.

597 Gao, B. C., Fang, W. P., Kong, X. X., Xu, J. M., Guan, Z. T., Yang, J. L., Xiong, J. H., Yi, T. P., Wu,
598 Y. T., Tan, and Z. M.: Flora of Sichuan, Sichuan People's Publishing House, Chengdu, 1981.
599 Guo, K., Fang, J. Y., Wang, G. H., Tang, Z. Y., Xie, Z. Q., Shen, Z. H., Wang, R. Q., Qiang, S., Liang,
600 C. Z., Da, L. J., and Yu, D.: A revised scheme of vegetation classification system of China,
601 Chin. J. Plant Ecol., 44, 111–127, https://doi.org/10.17521/cjpe.2019.0271, 2020.
602 He, Y. L., Xiong, Q. L., Yu, L., Yan, W. B., and Qu, X. X.: Impact of climate change on potential
603 distribution patterns of alpine vegetation in the Hengduan Mountains region, China, Mt. Res.
604 Dev., 40, R48–R54, https://doi.org/10.1659/MRD-JOURNAL-D-20-00010.1, 2020.
605 iFlora Initiative of Kunming Institute of Botany, Chinese Academy of Sciences: A Dictionary of the
606 Families and Genera of Chinese Vascular Plants, Science Press, Beijing, 2018.
607 Integrated Scientific Expedition to Qinghai-Tibet Plateau, Chinese Academy of Sciences: Flora
608 Xizangica, 5 volumes, Science Press, Beijing, 1983–1987.
609 Integrated Scientific Expedition to Qinghai-Tibet Plateau, Chinese Academy of Sciences: Physical
610 Geography of Hengduan Mountains, Science Press, Beijing, 1997.
611 Jin, Y. L., Wang, H. Y., Wei, L. F., Hou, Y., Hu, J., Wu, K., Xia, H. J., Xia, J., Zhou, B. R., Li, K.,
612 and Ni, J.: A plot-based dataset of plant community on the Qingzang Plateau, Chin. J. Plant
613 Ecol., 46, 846–854, https://doi.org/10.17521/cjpe.2022.0174, 2022.
614 Jin, Y. L., Yang, L. Y. Y., Hu, X. F., Yang, C., Xia, H. J., Hou, Y., Wu, K., Mao, X. X., Ni, J.: A plot-
615 based plant community dataset in the Hengduan Mountains (2022-2024), National Tibetan
616 Plateau / Third Pole Environment Data Center, https://doi.org/10.11888/Terre.tpdc.303394,
617 2026.
618 Jin, Z. Z.: The Features of Floras in the Dry-hot and Dry-warm Valleys in Yunnan and Sichuan
619 Provinces, Yunnan Science and Technology Press, Kunming, 2002.
620 Jin, Z. Z., and Ou, X. K.: Yuanjiang, Nujiang, Jinshajiang, Lancangjiang Vegetation of Dry Valley,
621 Yunnan University Press & Yunnan Science and Technology Press, Kunming, 2000.
622 Kunming Institute of Botany, Chinese Academy of Sciences: Flora of Yunnan, 21 volumes, Science
623 Press, Beijing, 1977–2006.
624 Li, D. J.: The primary characteristics of flora in the Hengduan Mountainous regions, Mt. Res., 6,
625 147–152, https://doi.org/10.16089/j.cnki.1008-2786.1988.03.003, 1988.
626 Li, X. W.: Floristic statistics and analyses of seed plants from China, Acta Bot. Yunnan., 18, 363–

https://doi.org/10.5194/essd-2026-204
Preprint. Discussion started: 1 April 2026
© Author(s) 2026. CC BY 4.0 License.

384, 1996.

Liang, Q. L., Xu, X. T., Mao, K. S., Wang, M. C., Wang, K., Xi, Z. X., and Liu, J. Q.: Shifts in plant distributions in response to climate warming in a biodiversity hotspot, the Hengduan Mountains, J. Biogeogr., 45, 1334–1344, https://doi.org/10.1111/jbi.13229, 2018.

Liu, Y., Li, P., Xu, Y., Shi, S. L., Ying, L. X., Zhang, W. J., Peng, P. H., and Shen, Z. H.: Quantitative classification and ordination for plant communities in dry valleys of Southwest China, Biodiv. Sci., 24, 378–388, https://doi.org/10.17520/biods.2015241, 2016a.

Liu, Y., Zhu, X. X., Shen, Z. H., and Sun, H.: Flora compositions and spatial differentiations of vegetation in dry valleys of Southwest China, Biodiv. Sci., 24, 367–377, https://doi.org/10.17520/biods.2015240, 2016b.

Myers, N., Mittermeier, R. A., Mittermeier, C. G., da Fonseca, G. A. B., and Kent, J.: Biodiversity hotspots for conservation priorities, Nature, 403, 853–858, https://doi.org/10.1038/35002501, 2000.

Nan, X., Li, A. N., and Deng, W.: Data set of "Digital Mountain Map of China" (2015), National Tibetan Plateau / Third Pole Environment Data Center, https://doi.org/10.11888/Terre.tpdc.272523, 2022.

Piao, S. L., Zhang, X. Z., Wang, T., Liang, E. Y., Wang, S. P., Zhu, J. T., and Niu, B.: Responses and feedback of the Tibetan Plateau's alpine ecosystem to climate change, Chin. Sci. Bull., 64, 2842–2855, https://doi.org/10.1360/TB-2019-0074, 2019.

Sabatini, F. M., Lenoir, J., Hattab, T., Arnst, E. A., Chytrý, M., Dengler, J., De Ruffray, P., Hennekens, S. M., Jandt, U., Jansen, F., Jiménez-Alfaro, B., Kattge, J., Levesley, A., Pillar, V. D., Purschke, O., Sandel, B., Sultana, F., Aavik, T., Aćić, S., Acosta, A. T. R., Agrillo, E., Alvarez, M., Apostolova, I., Arfin Khan, M. A. S., Arroyo, L., Attorre, F., Aubin, I., Banerjee, A., Bauters, M., Bergeron, Y., Bergmeier, E., Biurrun, I., Bjorkman, A. D., Bonari, G., Bondareva, V., Brunet, J., Čarni, A., Casella, L., Cayuela, L., Černý, T., Chepinoga, V., Csiky, J., Ćušterevska, R., De Bie, E., de Gasper, A. L., De Sanctis, M., Dimopoulos, P., Dolezal, J., Dziuba, T., El-Sheikh, M. A. E.-R. M., Enquist, B., Ewald, J., Fazayeli, F., Field, R., Finckh, M., Gachet, S., Galán-de-Mera, A., Garbolino, E., Gholizadeh, H., Giorgis, M., Golub, V., Alsos, I. G., Grytnes, J.-A., Guerin, G. R., Gutiérrez, A. G., Haider, S., Hatim, M. Z., Hérault, B., Hinojos Mendoza, G., Hölzel, N., Homeier, J., Hubau, W., Indreica, A., Janssen, J. A. M., Jedrzejek, B., Jentsch,

https://doi.org/10.5194/essd-2026-204
Preprint. Discussion started: 1 April 2026
© Author(s) 2026. CC BY 4.0 License.

A., Jürgens, N., Kącki, Z., Kapfer, J., Karger, D. N., Kavgacı, A., Kearsley, E., Kessler, M., Khanina, L., Killeen, T., Korolyuk, A., Kreft, H., Kühl, H. S., Kuzemko, A., Landucci, F., Lengyel, A., Lens, F., Lingner, D. V., Liu, H., Lysenko, T., Mahecha, M. D., Marcenò, C., Martynenko, V., Moeslund, J. E., Monteagudo Mendoza, A., Mucina, L., Müller, J. V., Munzinger, J., Naqinezhad, A., Noroozi, J., Nowak, A., Onyshchenko, V., Overbeck, G. E., Pärtel, M., Pauchard, A., Peet, R. K., Peñuelas, J., Pérez-Haase, A., Peterka, T., Petřík, P., Peyre, G., Phillips, O. L., Prokhorov, V., Rašomavičius, V., Revermann, R., Rivas-Torres, G., Rodwell, J. S., Ruprecht, E., Rūsiņa, S., Samimi, C., Schmidt, M., Schrodt, F., Shan, H., Shirokikh, P., Šibík, J., Šilc, U., Sklenář, P., Škvorc, Ž., Sparrow, B., Sperandii, M. G., Stančić, Z., Svenning, J.-C., Tang, Z., Tang, C. Q., Tsiripidis, I., Vanselow, K. A., Vásquez Martínez, R., Vassilev, K., Vélez-Martin, E., Venanzoni, R., Vibrans, A. C., Violle, C., Virtanen, R., von Wehrden, H., Wagner, V., Walker, D. A., Waller, D. M., Wang, H.-F., Wesche, K., Whitfeld, T. J. S., Willner, W., Wiser, S. K., Wohlgemuth, T., Yamalov, S., Zobel, M., and Bruelheide, H.: sPlotOpen – An environmentally balanced, open-access, global dataset of vegetation plots, Glob. Ecol. Biogeogr., 30, 1740–1764, https://doi.org/10.1111/geb.13346, 2021.

Shen, Z. H., Liu, Z. L., and Wu, J.: Altitudinal pattern of flora on the eastern slope of Mt. Gongga, Biodiv. Sci., 12, 89–98, https://doi.org/10.17520/biods.2004011, 2004.

Sherman, R., Mullen, R., Li, H. M., Fang, Z. D., and Wang, Y.: Spatial patterns of plant diversity and communities in alpine ecosystems of the Hengduan Mountains, northwest Yunnan, China, J. Plant Ecol., 1, 117–136, https://doi.org/10.1093/jpe/rtn012, 2008.

Sloan, S., Jenkins, C. N., Joppa, L. N., Gaveau, D. L. A., and Laurance, W. F.: Remaining natural vegetation in the global biodiversity hotspots, Biol. Conserv., 177, 12–24, https://doi.org/10.1016/j.biocon.2014.05.027, 2014.

Sun, H., Zhang, J. W., Deng, T., and Boufford, D. E.: Origins and evolution of plant diversity in the Hengduan Mountains, Plant Divers., 39, 161–166, https://doi.org/10.1016/j.pld.2017.09.004, 2017.

Wang, G. H., Fang, J. Y., Guo, K., Xie, Z. Q., Tang, Z. Y., Shen, Z. H., Wang, R. Q., Wang, X. P., Wang, D. L., Qiang, S., Yu, D., Peng, S. L., Da, L. J., Liu, Q., and Liang, C. Z.: Contents and protocols for the classification and description of vegetation formations, alliances and associations of vegetation of China, Chin. J. Plant Ecol., 44, 128–178,

https://doi.org/10.5194/essd-2026-204
Preprint. Discussion started: 1 April 2026
© Author(s) 2026. CC BY 4.0 License.

687 https://doi.org/10.17521/cjpe.2019.0272, 2020.
688 Wu, S. H., Pan, T., Cao, J., He, D. M., and Xiao, Z. N.: Barrier-corridor effect of longitudinal range-
689 gorge terrain on monsoons in Southwest China, Geogr. Res., 31, 1–13,
690 https://doi.org/10.11821/yj2012010001, 2012.
691 Wu, Z. Y.: The areal-types of Chinese genera of seed plants. Acta Bot. Yunnan., Suppl. IV, 1–139,
692 1991.
693 Wu, Z. Y., Zhou, Z. K., Li, D. Z., Peng, H., and Sun, H.: The areal-types of the world families of
694 seed plants, Acta Bot. Yunnan., 25, 245–257, 2003.
695 Xing, Y. W., and Ree, R. H.: Uplift-driven diversification in the Hengduan Mountains, a temperate
696 biodiversity hotspot, P. Natl. Acad. Sci. USA, 114, E3444–E3451,
697 https://doi.org/10.1073/pnas.1616063114, 2017.
698 Xu, B., Li, Z. M., and Sun, H.: Plant diversity and floristic characters of the alpine subnival belt
699 flora in the Hengduan Mountains, SW China, J. Syst. Evol., 52, 271–279,
700 https://doi.org/10.1111/jse.12037, 2014.
701 Xu, C. D., Feng, J. M., Wang, X. P., and Yang, X.: Vertical distribution patterns of plant species
702 diversity in northern Mt. Gaoligong, Yunnan Province, Chin. J. Ecol., 27, 323–330, 2008.
703 Yang, J. D., Zhang, Z. M., Shen, Z. H., Ou, X. K., Geng, Y. P., and Yang, M. Y.: Review of research
704 on the vegetation and environment of dry-hot valleys in Yunnan, Biodiv. Sci., 24, 462–474,
705 https://doi.org/10.17520/biods.2015251, 2016.
706 Yang, Q. Y. and Zheng, D.: An outline of physico-geographic regionalization of the Hengduan
707 Mountains region, Mt. Res., 7, 56–64, https://doi.org/10.16089/j.cnki.1008-2786.1989.01.010,
708 1989.
709 Yang, Y., Han, J., Liu, Y., Zhong-Yong, C. R., Shi, S. L., Si-Na, C. L., Xu, Y., Ying, L. X., Zhang,
710 W. J., and Shen, Z. H.: A comparison of the altitudinal patterns in plant species diversity within
711 the dry valleys of the Three Parallel Rivers region, northwestern Yunnan, Biodiv. Sci., 24, 440–
712 452, https://doi.org/10.17520/biods.2015361, 2016.
713 Yao, Y. H., Zhang, B. P., Han, F., and Pang, Y.: Diversity and geographical pattern of altitudinal belts
714 in the Hengduan Mountains in China, J. Mt. Sci., 7, 123–132, https://doi.org/10.1007/s11629-
715 010-1011-9, 2010.
716 Yin, L., Dai, E. F., Zheng, D., Wang, Y. H., Ma, L., and Tong, M.: What drives the vegetation

https://doi.org/10.5194/essd-2026-204
Preprint. Discussion started: 1 April 2026
© Author(s) 2026. CC BY 4.0 License.

717 dynamics in the Hengduan Mountain region, southwest China: climate change or human
718 activity?, Ecol. Indic., 112, 106013, https://doi.org/10.1016/j.ecolind.2019.106013, 2020.
719 Yu, H. B., Miao, S. Y., Xie, G. W., Guo, X. Y., Chen, Z., and Favre, A.: Contrasting floristic diversity
720 of the Hengduan Mountains, the Himalayas and the Qinghai-Tibet Plateau sensu stricto in
721 China, Front. Ecol. Evol., 8, 136, https://doi.org/10.3389/fevo.2020.00136, 2020.
722 Yu, Y. D., Liu, L. H., and Zhang, J. H.: Vegetation regionalization of the Hengduan Mountains region,
723 Mt. Res., 7, 47–55, https://doi.org/10.16089/j.cnki.1008-2786.1989.01.009, 1989.
724 Zhang, H. N., Zou, W., Chen, Z., He, L. J., Peng, X. F., Wang, G. Y., Peng, P. H., Li, J. J., and Shi,
725 S. L.: Distribution pattern of plant communities and its relationship with environmental factors
726 in eastern Xizang, China, Chin. J. Appl. Environ. Biol., 29, 1289–1297,
727 https://doi.org/10.19675/j.cnki.1006-687x.2022.10037, 2023.
728 Zhang, R. Z., Zheng, D., Yang, Q. Y., and Liu, Y. H.: Physical Geography of Hengduan Mountains,
729 Science Press, Beijing, 1997.
730 Zhang, S.R.: Carex. In: Hong, D.Y., Sun, H., Watson, M., Wen, J., Zhang, X.C. (eds), Flora of Pan-
731 Himalaya, Vol. 12, Science Press, Beijing, 2020.
732 Zhang, X. Q., Xu, X. M., Li, X., Cui, P., and Zheng, D.: A new scheme of climate-vegetation
733 regionalization in the Hengduan Mountains region, Sci. China Earth Sci., 67, 751–768,
734 https://doi.org/10.1007/s11430-023-1231-0, 2024.
735 Zhang, X. Z., Yang, Y. P., Piao, S. L., Bao, W. K., Wang, S. P., Wang, G. X., Sun, H., Luo, T. X.,
736 Zhang, Y. J., Shi, P. L., Liang, E. Y., Shen, M. G., Wang, J. S., Gao, Q. Z., Zhang, Y. L., and
737 Ouyang, H.: Ecological change on the Tibetan Plateau, Chin. Sci. Bull., 60, 3048–3056,
738 https://doi.org/10.1360/N972014-01339, 2015.
739 Zheng, D.: A comparative study on physico-geographic conditions between the Himalayas and
740 Hengduan Mountainous regions, Mt. Res., 6, 137–144, 1988.
741 Zheng, D. and Yang, Q. Y.: Some problems on physicogeographic regionalization of the Hengduan
742 Mountains region, Mt. Res., 5, 7–13, 1987.